

Heat treatment effect on structure and atomic composition in the outermost surface layer of $\text{La}_2\text{O}_3\text{-TiO}_2\text{-SiO}_2$ system

A. CHENITI, O. PONTA, L. TIRLE, T. RADU, S. SIMON*

Babes-Bolyai University, Faculty of Physics & Institute for Interdisciplinary Research in Bio-Nano-Science, Cluj-Napoca, 400084, Romania

The influence of isochronous heat treatments applied at different temperatures between 350 °C and 1100°C, under the same conditions and schedules, on 50 La_2O_3 -25 TiO_2 -25 SiO_2 microparticles prepared by spray drying was investigated by scanning electron microscopy, X-ray diffraction and X-ray induced photoelectron spectroscopy. Differences in the elemental composition on outermost layer of the samples treated at different temperatures are observed. Major changes are obtained after the heat treatment carried out at 1100°C. Treatment temperatures above 700 °C promote the nucleation and growth of La_2O_3 , TiO_2 , La_2TiO_5 and $\text{La}_{9.33}\text{Si}_6\text{O}_{26}$ nanocrystallites. The highest lanthanum and silicon content occur on the surface of 1100°C treated sample and is related to prevalent development of $\text{La}_{9.33}\text{Si}_6\text{O}_{26}$ nanocrystalline phase.

(Received February 23, 2012; accepted June 5, 20102)

Keywords: Lanthanum, Titania, Silica, Spray drying, XPS

1. Introduction

High content lanthanum systems in oxyapatite structures with silica, but also with other oxides, attracted large interest especially for catalysis applications [1, 2]. The synthesis of $\text{La}_2\text{O}_3\text{-TiO}_2\text{-SiO}_2$ glass system by the conventional melting method was not reported as far, but the system was successfully prepared using the sol-gel route [3]. A lot of compounds of apatite type structures, with general formula $\text{X}_{10}(\text{ZO}_4)_6\text{O}_2$, or $\text{X}_{10}\text{Z}_6\text{O}_{26}$, had been synthesised by sol-gel method [4-7].

Titanium addition proved the possibility to synthesise high-oxygen-content silicate-based apatites, with effects on their conductivity, that is related to trapping of the interstitial oxide ions around the titanium atoms. Similar compositions containing lanthanum cation vacancies promote the tendency to form $\text{La}_2\text{Ti}_2\text{O}_7$ phase [2]. At the same time, it was reported that lanthanum enhances in vitro osteoblast differentiation but has no effect on type I collagen [7]. Interestingly, lanthanum is rapidly emerging as a major player in the management of multiple other different systemic diseases especially in the field of oncology [8-12]. The effect of rare earths addition on hydrophilicity of $\text{TiO}_2/\text{SiO}_2$ films was also reported, namely that the hydrophilicity of pure TiO_2 film is enhanced by both SiO_2 and La_2O_3 or Ce_2O_3 [13].

Nevertheless, it was also signalized the cytotoxic and genotoxic effect of lanthanum nitrate on human lymphocytes, if accumulated in the body [12]. It was assumed that many of these toxic effects arise from the ability of Ln^{3+} ions to replace Ca^{2+} isomorphously or antagonize Ca^{2+} in a variety of cellular and sub cellular reactions [14]. Recently were published results on the

acute functional neurotoxicity of lanthanum(III) in primary cortical networks using LaCl_3 [15]. The study demonstrated inhibitory and potentially sedative toxicological effects of lanthanum(III) ions at concentrations comparable to the plasma concentrations observed in patients with kidney diseases treated with lanthanum carbonate for hyperphosphatemia. Therefore, given the lack of proof that the blood-brain barrier is completely impermeable in uremic patients and lanthanum cannot cross, caution is warranted.

Because of its diverse physical and chemical properties, lanthanum has been used in various industrial and medical fields. Not only lanthanum, but lanthanides, because of their diversified physical and chemical effects, have been widely used in a number of fields. As a result, more and more lanthanides are entering into the environment and eventually accumulated in human body [16].

The release of lanthanum in different environments depends on lanthanum occurrence on the surface of the samples, with respect to both concentration and structural bonds. X-ray Photoelectron Spectroscopy (XPS) is successfully used for chemical analysis on the samples surface that conferred to XPS method also the designation Electron Spectroscopy for Chemical Analysis (ESCA). In fact, XPS is an important technique for investigation of electronic structure and chemical bonding in solids as well as in describing the local structure [17].

The aim of this study was to investigate the heat treatment influence on the composition in the surface layer of $\text{La}_2\text{O}_3\text{-TiO}_2\text{-SiO}_2$ microparticles because their physical and chemical surface properties are of major interest in different applications.

2. Experimental

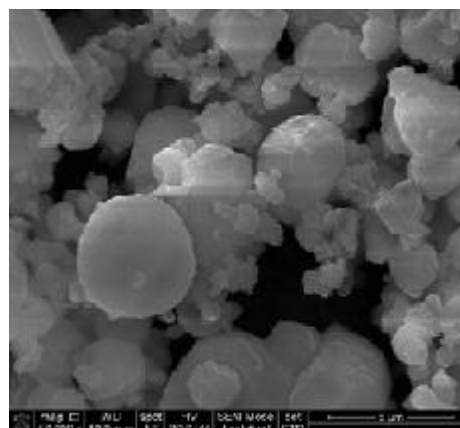
Microparticles with $50\text{La}_2\text{O}_3\cdot 25\text{TiO}_2\cdot 25\text{SiO}_2$ composition, doped with 1% Gd_2O_3 , were prepared using the spray drying method by means of Buchi-290 Mini Spray-dryer. The precursors for the synthesis of the sol-gel intermediate phase were lanthanum nitrate hexahydrate $\text{LaN}_3\text{O}_9\cdot 6\text{H}_2\text{O}$, titanium isopropoxide $\text{C}_{12}\text{H}_{28}\text{O}_4\text{Ti}$, tetraethoxysilane $\text{Si}(\text{OC}_2\text{H}_5)_4$ (TEOS), and gadolinium nitrate hexahydrate $\text{Gd}(\text{NO}_3)_3\cdot 6\text{H}_2\text{O}$. The as prepared samples were heat treated in air, under normal pressure, at increasing temperatures ranging from 350 °C to 1100 °C, for 30 minutes.

The samples morphology was examined with a scanning electronic microscope (SEM) – FEI QUANTA 3D FEG dual beam, in high vacuum work mode using ETD - Everhart Thornley Detector. The structure of the samples was analysed by X-ray diffraction (XRD). The XRD patterns were recorded with a Shimadzu XRD – 6000 diffractometer using $\text{Cu K}\alpha$ ($\lambda = 1.5405 \text{ \AA}$) radiation. Crystallographic identification was accomplished by comparing the experimental XRD patterns with JCPDS standard inorganic crystal structure data.

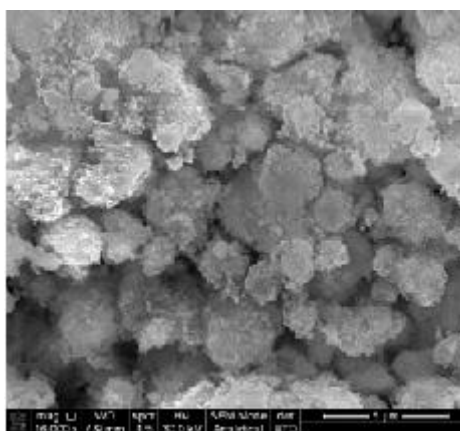
The elemental composition in the outermost layer of the microparticles after treatments carried out at different temperatures was determined by X-ray photoelectron spectroscopy (XPS) measurements using a SPECS PHOIBOS 150 MCD spectrometer with monochromatic $\text{AlK}\alpha$ source (150 W, $h\nu = 1486.74 \text{ eV}$). A low energy electron beam was used to achieve charge neutrality at the sample surface. XPS survey spectra were recorded with a pass energy of 100 eV, over the binding energy range 0–1200 eV. The binding energies were referenced to the C 1s photoelectron peak at 284.6 eV that usually results on all surfaces exposed to the atmosphere as adsorbed species. The analysis of the data was performed with CasaXPS software.

3. Results and discussion

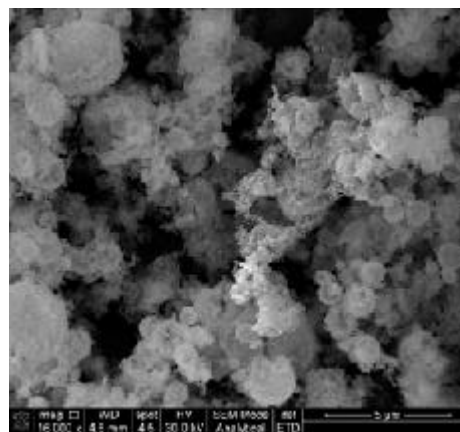
The spray dried samples consists of microparticles below 5 μm in size (Fig. 1). By heat treatment of the as prepared samples (Fig. 1a), the particles size occur diminished (Fig. 1b and c) due both to removal of water and alcohols molecules still resident in spray dried samples [18, 19] and to densification and structural changes [20, 21]. An enhanced particles agglomeration is observed with increasing treatment temperature.



(a)



(b)



(c)

Fig. 1. SEM images of (a) as prepared, heat treated at 800 °C (b) and (c) 1100 °C microparticles (the scale bars are 5 μm).

The XRD analysis reveals that the heat treated samples are amorphous up to 700 °C treatment temperatures (Fig. 2). In case of amorphous systems obtained by melting, their properties are controlled by the composition of the melt and atomic-scale structure, including cation coordination environments [22] and these would have to be considered also for sol-gel derived systems. The composition of a glass has a large effect on the amount of high coordinated species formed. In the investigated $50\text{La}_2\text{O}_3\text{-}25\text{TiO}_2\text{-}25\text{SiO}_2$ system the number of lanthanum ions which are non-network cations highly exceeds the number of Si^{4+} and Ti^{4+} ions with network former ability, of high cation field strength (charge divided by the square of ionic radius). This explains the difficulty to prepare such a composition in vitreous state using the melting method. The ionic radius, coordination type, ionic field strength, single bond strength with oxygen and electronegativity of the cations entering in the investigated glasses are given in Table 1. With respect to the electronegativity values, they clearly differ from each other. On the other hand, one remarks that for La^{3+} and Si^{4+} ions the M-O bond strengths are close.

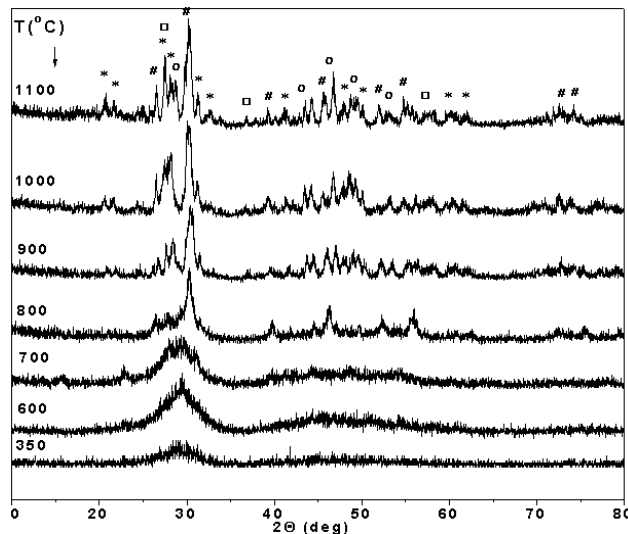


Fig. 2. XRD patterns recorded from samples treated at different temperatures (\square TiO_2 , \circ La_2TiO_5 , $*$ $\text{La}_{9.33}\text{Si}_6\text{O}_{26}$, $\#$ La_2O_3).

Table 1. Ionic radius, coordination type, cation field strength, single bond strength with oxygen and electronegativity of the cations entering in the investigated samples.

Cation	Coord. type	Shannon ionic radius [23,24] (Å)	Cation field strength (Å ⁻²)	M-O bond strength [25] kJ/mol	Pauling electroneg. [25]
La^{3+}	6	1.17	2.19	799 ± 4	1.1
	8	1.30	1.78		
Si^{4+}	4	0.40	25	799.6 ± 13.4	1.90
	6	0.54	13.72		
	8	0.88	5.17		
Ti^{4+}	4	0.56	12.76	672.4 ± 9.2	1.54
	6	0.75	7.11		
	8	0.88	5.17		

Starting with 700 °C treatment, a nucleation process is observed that will develop crystallites clearly evidenced at higher temperatures (Fig. 2). The XRD pattern of the microparticles treated at 800 °C reveals the development of La_2O_3 (JCPDS no.74-1144) nanocrystals in the amorphous matrix. The crystallites size determined with Scherrer equation is about 2 nm. After 900 °C treatment, La_2TiO_5 (JCPDS no. 75-2394) nanocrystals are also developed. Starting with 1000 °C treatment, the nucleation and growth of $\text{La}_{9.33}\text{Si}_6\text{O}_{26}$ (JCPDS no. 49-0443) nanocrystalline phase is evidenced, while in 1100 °C treated sample are also present TiO_2 (JCPDS no. 21-1272) nanocrystals. The decrease of the crystallisation temperature in sol-gel derived samples, in comparison to the conventional methods, and obtaining of nanocrystalline particles is a main advantage [26]. Lower crystallisation temperatures of phases including the apatite structure were also reported for samples prepared by sputtering methods [27].

ESCA results obtained from XPS survey spectra (Fig. 3) are summarized in Table 2. The composition was computed by neglecting the carbon assigned to contamination.

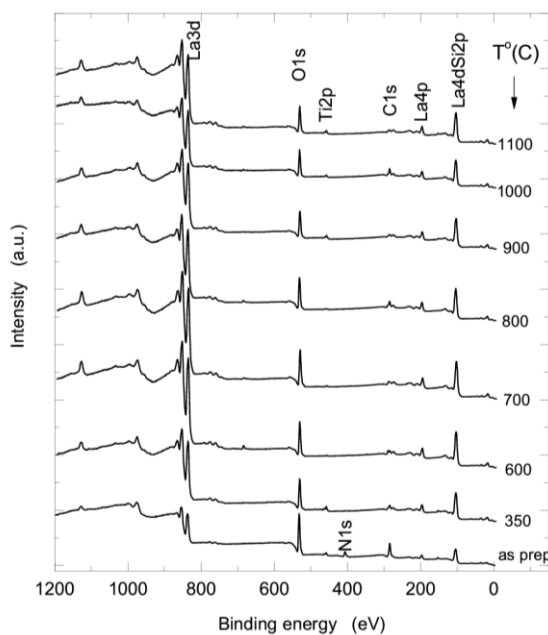


Fig. 3. XPS survey spectra recorded from samples treated at different temperatures.

Table 2. The elemental composition (at %) on outermost surface layer of the microparticles before and after thermal treatment at different temperature.

Treatment temp. (°C)	Elements					Si/Ti
	O	La	Si	Ti	N	
as prepared	67	8.4	7.1	2.1	15.5	3.4
350	68.3	20.1	7.5	4.1		1.8
600	73.5	25.7	0.4	0.3		1.3
700	73	25.3	1	0.5		2
800	73.9	24.7	0.6	0.5		1.2
900	67.1	24.5	4.5	3.9		1.2
1000	66.1	24.9	4.4	3.3		1.3
1100	63.9	26.1	6.8	3.2		2.1

Nitrogen occurs in the as prepared sample from the nitrates used as precursors in sol-gel synthesis and will be removed already after 350 °C treatment. On all samples surface the Si/Ti ratio is higher than 1. The highest lanthanum and silicon content occur on the surface of 1100°C treated sample and is related to development of La_{9,33}Si₆O₂₆ nanocrystalline phase.

4. Conclusions

50La₂O₃·25TiO₂·25SiO₂ microparticles less than 5 µm in size were prepared using the spray drying method. The heat treatments applied between 350 °C and 1100 °C on the as-prepared particles induced changes in the elemental composition on the particles surface. Treatment temperatures above 700 °C promote the nucleation and growth of La₂O₃, TiO₂, La₂TiO₅ and La_{9,33}Si₆O₂₆ nanocrystallites. This decrease of the crystallisation temperature in spray dried samples, in comparison to the samples prepared by conventional melting method, is an important advantage. The highest lanthanum and silicon content occur on the surface of 1100°C treated sample and is related to development of La_{9,33}Si₆O₂₆ apatite type nanocrystalline structures. On all samples surface the Si/Ti ratio is higher than 1.

Acknowledgements

This research was accomplished in the framework of PNII Idei PCCE-101/2008 project granted by the Romanian National University Research Council - CNCSIS.

References

- [1] X.-H. Zhang, X. Yi, J. Zhang, Z. Xie, J. Kang, L. Zheng, *Inorg. Chem.* **49**, 10244 (2010).
- [2] A. Al-Yasari, A. Jones, A. Orera, D.C. Apperley, D. Driscoll, M. S. Islam, P. R. Slater, *J. Mater. Chem.* **19**, 5003 (2009).
- [3] M. Iwasaki, H. Masaki, S. Ito, W.-K. Park, *J. Kor. Ceram. Soc.* **44**, 137 (2007).
- [4] L.-C. Leu, S. Thomas, M. T. Sebastian, S. Zdzieszynski, S. Misture, R. Ubic, *J. Am. Ceram. Soc.* **94**, 2625 (2011).
- [5] T. Kinoshita, T. Iwata, E. Bechade, O. Masson, I. Julien, E. Champion, P. Thomas, H. Yoshida, N. Ishizawa, K. Fukuda, *Solid State Ionics* **181**, 1024, (2010).
- [6] R. Ali, M. Yashima, Y. Matsushita, H. Yoshioka, F. Izumi, *J. Solid State Chem.* **182**, 2846 (2009).
- [7] X. Wang, L. Yuan, J. Huang, T.-L. Zhang, K. Wang, *J. Cell. Biochem.* **105**, 1307 (2008).
- [8] S. Kapoor, *J. Cell. Biochem.* **106**, 193 (2009).
- [9] L. Feng, H. Xiao, X. He, Z. Li, F. Li, N. Liu, Z. Chai, Y. Zhao, Z. Zhang, *Neurotoxicol. Teratol.* **28**, 119 (2006).
- [10] G. Fei, L. Yuanlei, W. Yang, X. An, L. Guohui, *J. Rare Earths* **25**, 359 (2007).
- [11] L. Bernard, L. Anthony, A. Daniel, R. Nadya, M. Natalie, B.D. Tilman, *Kidney Int.* **67**, 1062 (2005).
- [12] A. V. Paiva, M. S. de Oliveira, S. N. Yunes, L. G. de Oliveira, J. B. Cabral-Neto, C. E. B. de Almeida, *Bull. Environ. Contam. Toxicol.* **82**, 423 (2009).
- [13] K.-S. Guan, Y.-S. Yin, *Mater. Chem. Phys.* **92**, 10 (2005).
- [14] A. Palasz, P. Czekaj, *Acta Biochim. Pol.* **47**, 1107 (2000).
- [15] A. Gramowski, K. Jügelt, O. H.-U. Schröder, D.G. Weiss, S. Mitzneri, *Toxicol. Sci.* **120**, 173 (2011).
- [16] L. Feng, H. Xiao, X. He, Z. Li, F. Li, N. Liu, Y. Zhao, Y. Huang, Z. Zhang, Z. Chai, *Toxicol. Lett.* **165**, 112 (2006).
- [17] G. D. Khattak, N. Tabet, L. E. Wenger, *Phy. Rev. B* **72**, 1 (2005).
- [18] B. Alonso, E. Veron, D. Durand, D. Massiot, C. Clinard, *Micropor. Mesopor. Mater.* **106**, 76 (2007).
- [19] M. Todea, R. V. F. Turcu, B. Frentiu, M. Tamasan, H. Mocuta, O. Ponta, S. Simon, *J. Mol. Struct.* **1000**, 62 (2011).
- [20] M. Balasubramanian, S. K. Malhotra, C. V. Gokularathnam, *J. Nater. Sci.* **30**, 3515 (1995).
- [21] A. Pilarska, E. Markiewicz, F. Ciesielczyk, T. Jesionowski, *Dry. Technol.* **29**, 1210 (2011).
- [22] K. E. Kelsey, J. F. Stebbins, D. M. Singer, G. E. Brown Jr., J. L. Mosenfelder, P. D. Asimow, *Geochim. Cosmochim. Acta* **73**, 3914 (2009).
- [23] R. D. Shannon, *Acta Cryst. A* **32**, 751 (1976).
- [24] J. E. Huheey, E. A. Keiter, R. L. Keiter in *Inorganic Chemistry: Principles of Structure and Reactivity*, 4th edition, HarperCollins, New York, USA, 1993.
- [25] J. A. Kerr in *CRC Handbook of Chemistry and Physics*, D. R. Lide, (ed.) CRC Press, Boca Raton, Florida, USA, 81-st ed., 2000.
- [26] S. Celerier, C. Laberty-Robert, F. Ansart, C. Calmet, P. Stevens, *J. Eur. Ceram. Soc.* **25**, 2665 (2005).
- [27] G. E. Stan, *J. Optoelectron. Adv. Mater.* **11**, 1132 (2009).

*Corresponding author: simion.simon@phys.ubbcluj.ro